Accelerated Pyrolysis Analysis of Thick High-Temperature Composite Parts Using Theory-Guided Probabilistic Machine Learning and Finite Element Analysis

Paulina Portales Picazo; Derrick Ong; Alexander Gray; Navid Zobeiry

OFFICIAL CONFERENCE PUBLICATION

Proceedings of the American Society for Composites - Thirty-Eighth Technical Conference (2023)

https://doi.org/10.12783/asc38/36579

RELATED SUBSTANTIALLY EXTENDED JOURNAL ARTICLE

P. Portales Picazo, A. Gray, and N. Zobeiry, "Efficient Characterization and Optimization of Pyrolysis in Carbon-Carbon Composites Through Machine Learning," Composites Part A 190, 108664 (2025).

https://doi.org/10.1016/j.compositesa.2024.108664

ABSTRACT

Fabrication of advanced composites for high-temperature applications typically involves a complex, multi-step process. This process includes an initial lay-up step, curing, high-temperature pyrolysis to transform the cured resin into a carbonized amorphous structure, several resin-backfilling steps to fill voids and cracks formed during pyrolysis, additional pyrolysis-densification cycles to further increase the carbon content, and a final graphitization step to achieve the desired crystalline structure of carbon atoms. The processing parameters in each step, as well as the lay-up and overall thickness of the part, directly impact the kinetics of reactions, phase transformations, and the resulting end-part properties. During pyrolysis, the resin undergoes a complex system of degradation reactions affected by heat and mass transfer through the part thickness. To achieve optimal performance of high-temperature composites, it is crucial to accurately establish the relationship between processing conditions, part geometry, and end-part properties. Current process optimization relies heavily on time-consuming and resource-intensive testing campaigns to characterize pyrolysis kinetics, followed by trial-and-error efforts. This is further complicated by complex temperature cycles, gradients of pyrolysis rate across thick composite parts, uncertainties, and variabilities of the material and process. This paper introduces a novel framework combining theory-guided probabilistic machine learning (ML) and finite element (FE) process simulation to address these challenges. Limited targeted experiments are used to characterize pyrolysis kinetics using an in-house developed ML code while quantifying uncertainty at each testing step. The kinetics model is then used by an FE model to simulate heat transfer and rate of pyrolysis, allowing the gradient of degree of pyrolysis across the thickness of a laminate to be simulated. For validation, laminates of varying thicknesses were fabricated and pyrolyzed using different temperature cycles. Imaging techniques including light microscopy and scanning electron microscopy (SEM) were utilized to capture the resulting microstructures.

Paulina Portales Picazo[1], Derrick Ong[1], Alexander Gray[1], Navid Zobeiry[1]
[1]Materials Science & Engineering, University of Washington, 302 Roberts Hall, Seattle, WA 98195, U.S.A.

An image analysis code was developed to detect cracks and voids to identify potential gradients and patterns. This, along with Raman spectroscopy, was used to estimate the degree of mass loss across the thickness of different parts and compared with predictions of the combined ML-FE framework. This framework significantly reduces trial-and-error experimental efforts and enables pyrolysis process optimization of thick composites to achieve desired properties, such as yield, porosity, and laminate permeability.

INTRODUCTION

Carbon-carbon composites, fabricated from fiber-reinforced polymer composites as the base material, are commonly used in high-temperature structural applications [1,2]. Throughout their manufacturing process, these materials undergo a series of complex reactions and phase transformations that yield a distinctive combination of mechanical, chemical, and thermal properties. These properties, including low density, high strength, and low ablation, are maintained at high temperatures, making these materials ideal for withstanding extreme thermo-mechanical conditions [1-4].

The efficient fabrication and optimal performance of these materials rely on accurately establishing the correlation between processing conditions, part geometry, and end-part properties [5]. In particular, the microstructural development occurring during the high-temperature pyrolytic process has a significant impact on the mechanical end-part properties [6]. This is due to the complex system of degradation reactions that the matrix undergoes during pyrolysis, which are influenced by heat and mass transfer across the part thickness and are therefore dependent of both the processing conditions and sample dimensions [7].

Current process optimization relies heavily on time-consuming and resource-intensive testing campaigns to characterize pyrolysis kinetics, followed by trial-and-error methods. The vast number of possible combinations for processing conditions, combined with the time-consuming testing process, results in an intractable search space limited by industry knowledge and experience. This is further complicated by complex temperature cycles, gradients of pyrolysis rate across thick composite parts, uncertainties, and variabilities of the material and process [8]. This paper introduces a novel framework combining theory-guided probabilistic machine learning (ML) and finite element (FE) process simulation to address these challenges.

The presented framework uses limited targeted experiments to characterize the pyrolysis kinetics using an in-house developed ML model, developed based on the underlying physics of pyrolysis, while quantifying uncertainty at each testing step [8,9]. The trained kinetics model is then utilized in conjunction with established theory in a 1D FE model to perform thermochemical analysis, determining heat transfer and rate of pyrolysis. This allows simulation of the gradient of degree of the pyrolysis throughout the thickness of a laminate for specific processing conditions and part geometry. Validation is done by using experimental methods such as cross-sectioning and image analysis, as well as density measurements of samples with various thicknesses.

By employing this framework, the need for trial-and-error experimental efforts is significantly reduced, enabling the optimization of the pyrolytic process for thick composites to achieve desired properties, such as yield and porosity.

MATERIALS AND METHODS

SAMPLE PREPARATION

The samples studied in this paper were fabricated using a proprietary carbon/phenolic resin-based prepreg system. Composite panels of different thicknesses, 0.64 cm (1/4'') and 1.3 cm (1/2''), were fabricated using quasi-isotropic lay-ups of $[(0/90)/(\pm 45)]_{8S}$ and $[(0/90)/(\pm 45)]_{16S}$ respectively, following the lay-up and bagging techniques recommended by the manufacturer. The composite laminates were then cured using an autoclave following the manufacturer's process specifications for pressure and temperature. The microstructure of the laminates was examined, and density measurements were conducted to characterize the laminates. The obtained results were consistent with the findings reported in relevant literature for similar systems. Samples were taken from the cured laminates for use in pyrolysis analysis using both thermogravimetric analysis (TGA) and a tube furnace setup designed specifically for this process. Samples had nominal dimensions of 0.2 × 0.1 × 0.64 cm and 3.9 x 3.8 x 1.3 cm; and weighed in the range of 8-10 mg, and 26-29 g respectively. An additional sample with dimensions of 1.4 x 4.1 x 0.64 cm and an initial weight of 14.17 g was trimmed for comparison and model validation. All samples used in this study were obtained from the mentioned laminates and subjected to the same storage conditions to minimize variability.

THERMOGRAVIMETRIC ANALYSIS

The degradation reactions occurring during the pyrolytic process were investigated using a TA Instruments TGA 550 Thermogravimetric Analyzer (TGA) equipment. The experiments were performed under a continuous flow of nitrogen gas (20 ml/min) introduced into the sealed TGA chamber. Open high-temperature platinum pans from TA instruments were used to hold the samples [10,11]. Weight-loss measurements and associated weight-loss rates were obtained and analyzed to examine the material's thermal stability and understand the kinetics of pyrolysis.

To ensure comprehensive analysis, the tests were conducted from room temperature to 1000°C and held isothermally for 20 minutes before cooling. This range was selected based on previous research indicating that similar polymeric matrices typically undergo pyrolytic reactions up to 800°C [3]. A total of 7 experiments were performed, employing various temperature cycles including single and multiple heating ramps (i.e., dynamic tests), as well as cycles with multiple ramps combined with isothermal holds. Smoothed weight loss and derivative weight loss curves corresponding to three example cycles are shown in Fig. 1:

- Heat-up from 200°C to 1000°C at a heating rate of 1°C/min, followed by a 20-minute hold.
- Heat-up from 200°C to 500°C at a heating rate of 2°C/min, followed by heating to 1000°C at a heating rate of 3°C/min, followed by a 20-minute hold.
- Heat-up from 200°C to 550°C at a heating rate of 5°C/min, followed by an hour hold, followed by heating to 1000°C at a heating rate of 2°C/min, followed by a 20-minute hold.

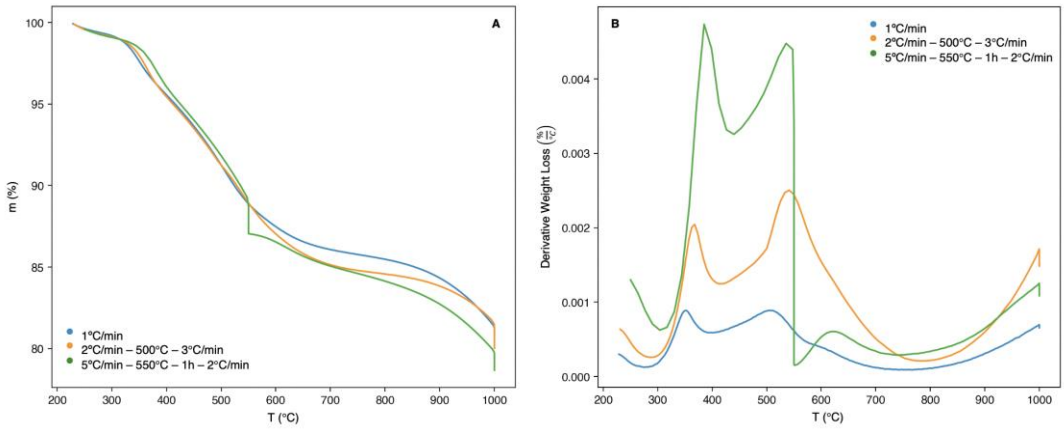

Figure 1. TGA weight loss (A), and derivative weight loss (B) curves of the cured composite panel at different heating rates.

HIGH-TEMPERATURE PYROLYTIC PROCESS

A tube furnace system was assembled and employed to investigate the high-pyrolytic process of the material and evaluate the influence of sample thickness on the extent of pyrolysis.

Following the recommendations given by the manufacturer, a multi-ramp temperature cycle with isothermal holds, ranging from room temperature to 1000°C, was employed for this experiment. Laminate samples of two different thicknesses, 0.64 cm (¼'') and 1.3 cm (½''), were subjected to this cycle. Samples were placed on slim alumina rods measuring 0.32 cm (⅛'') in thickness to minimize airflow obstruction at the bottom of the sample, and a continuous flow of nitrogen gas was introduced into the tube from one end to prevent oxidative degradation reactions throughout all the experiments [10,11].

The pyrolyzed samples were subjected to further analysis, and the obtained results were used for model validation.

Theory-Guided Machine Learning

DATA PROCESSING

Data acquired from TGA experiments were processed using Python and MATLAB codes to filter, smooth, and minimize noise. A theory-based outlier detection method was implemented to ensure the accuracy and reliability of the data used for training the machine learning (ML) model, and weight loss data related to polymerization and dewatering reactions during cure were removed by scaling the weight loss percentage to zero at 225°C [3].

The processed data was transformed based on the underlying theory of the pyrolysis process and established kinetics models prior to training ML models to ensure proper training while working with small datasets and to allow for extrapolation beyond the training zones [12-14]. The kinetics of the process and the

final char yield of each test were characterized by calculating the conversion rate or degree of pyrolysis (DOP), α, using the following expression [15]:

$$\alpha = \frac{m_i - m_t}{m_i - m_f} \quad (1)$$

where m_i and m_t denote the initial measured weight and the measured weight at time t, respectively, while m_f represents the minimum final measured weight across all experiments [15]. To ensure a consistent reference point and enable comparison of final yields obtained from various temperature cycles, the conversion rate α for each test was determined by employing a fixed minimum final weight fraction of 40% [8,9].

The expressions shown below were used to transform the test data based on the general form of the Arrhenius equation and the kinetics inherent to the pyrolytic process [8,15,16], before training ML models:

$$\frac{1}{T}\ ;\ \beta \times \ln(\alpha)\ ;\ \ln\left(\frac{d\alpha}{dt}\right)$$

where β denotes the temperature differential over time (dT/dt). These transformations ensure physical consistency in the trained ML model (i.e., theory-guided approach).

ML MODEL TRAINING

Gaussian Process Regression (GPR) was used in combination with the transformed data to train an accurate ML-based kinetic model of the high-temperature pyrolytic process [12,17-19]. The model was trained using cycles with different heating rates including single-ramp, multi-ramp, and multi-ramp with isothermal holds; and a combination of Radial Basis Function (RBF) was used as the kernel or covariance function [8,9,17]. The resulting mean surrogate surface obtained with these data, as well as several superposed experiments, are shown in Figure 2.

Obtained train and test scores for this model were 99.4% and 98.8% respectively. Model accuracy was verified by predicting the final yield for multiple temperature cycles and comparing it with the experimental results. In all cases, an error of less than 2% was observed, confirming the model's accuracy for its intended application [9].

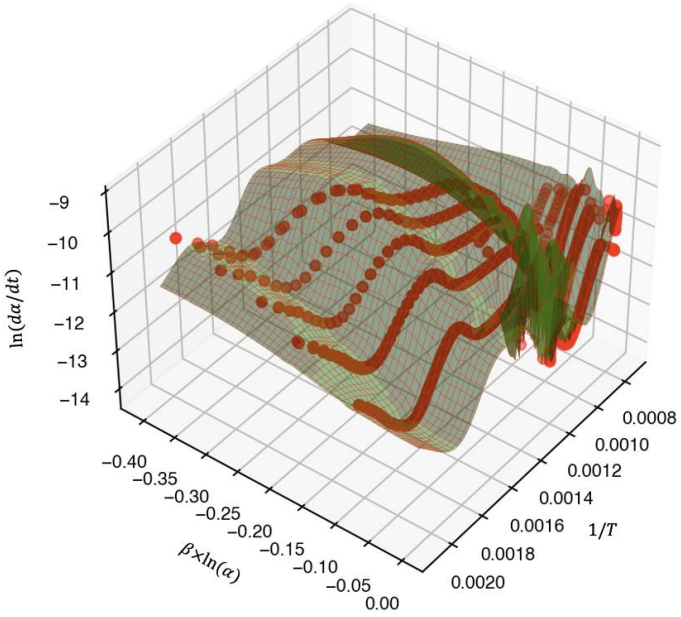

Figure 2. Mean surrogate surface of the trained ML kinetic model.

1D Finite Element Process Simulation

The 1D finite element (FE) process analysis method was utilized to simulate temperature, weight loss, and degree of pyrolysis (DOP) gradients across the thickness of the examined laminate during the high-temperature pyrolytic process from the pyrolysis kinetic ML-model.

An in-house Python program was adapted to the specific process, with the simulation inputs including the air temperature cycle, sample and tool thicknesses, and the estimated heat transfer coefficients at the top and bottom of the sample. The simulation also incorporated experimental observations and reported material properties, including density, thermal conductivity, and specific heat capacity of both the fibers and the polymeric matrix while considering the influence of their corresponding volume fractions and their evolution throughout the process.

A decrease in the matrix volume fraction, proportionate to the weight loss percentage, was assumed for the calculation of the composite density and thermal conductivity by obtaining the weight loss associated with the polymeric matrix at all times. The composite's specific heat capacity (Cp_C) was calculated using Eq. 2. In this calculation, the matrix density already accounted for the change in the matrix volume fraction.

$$Cp_C = \frac{\rho_m(\alpha) * Cp_m * Vf_m + \rho_f * Cp_f * Vf_f}{\rho_m(\alpha) * Vf_m + \rho_f * Vf_f} \quad (2)$$

Where Vf_m, Cp_m and Vf_f, Cp_f are the volume fractions and specific heat capacity of the matrix and fibers, respectively; and $\rho_m(\alpha)$ represents the matrix's density as a function of the conversion rate. No weight loss associated with the fiber

was considered; therefore, the properties corresponding to the fibers were assumed to remain constant.

These properties were used by the FE model to solve the coupled one-dimensional governing equations for heat transfer in the system, considering both conduction and convection mechanisms, as well as weight loss due to pyrolysis. The FE analysis was conducted by dividing both the tool and part thicknesses into 10 elements each.

To conduct a comprehensive analysis, different scenarios were simulated for the same temperature cycle and top heat transfer coefficient ($25\frac{W}{m^2K}$) by adjusting the part and tool thicknesses, as well as the heat transfer coefficient at the bottom of the samples. Mass transfer mechanism across the thickness was neglected in these simulations. Simulations were conducted for samples with thicknesses of 0.64 cm (¼''), 1.3 cm (½'') and 2.54 cm (1''). For each sample thickness, tool thicknesses of 1 cm and 0.5 cm were tested, with corresponding adjustments of the airflow at the bottom ranging from $5\frac{W}{m^2K}$ to $20\frac{W}{m^2K}$.

Figure 3 depicts the process setup schematic, highlighting key process variables.

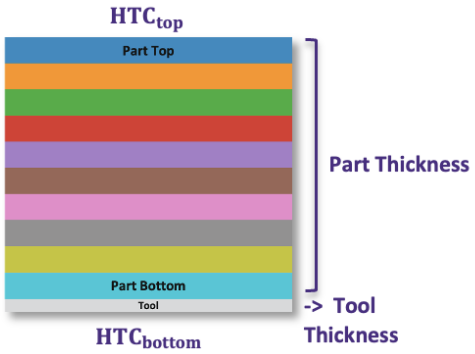

Figure 3. Schematic of the FE simulation setup.

Microstructure Analysis

Various characterization techniques were used to analyze and determine the microstructural properties of the composite laminates before and after pyrolysis. The resulting data was utilized to validate and enhance the ML algorithm previously discussed. The techniques and methods used are discussed next.

OPTICAL MICROSCOPY

Optical microscopy was used to capture images of the composite for analyzing the microstructure development and determining porosity percentage. Small cubic centimeter-sized samples of pyrolyzed and cured composites at 0.64 cm (¼") and 1.3 cm (½") thicknesses were cut . The samples were mounted under vacuum using a low-density potting resin, and then polished.

Using an Olympus BX-50 optical microscope, images of the samples at 5x, 10x, and 20x magnifications were obtained at different locations across the composite thickness. These magnifications were selected due to their resolution and level of detail when analyzed with computer vision.

Image analysis via Python scripts was performed on the optical microscopy images to determine the porosity of the sample at the imaged location. Using the OpenCV computer vision Python library, images were cropped to remove image artifacts and converted to grayscale. The pixel values of the resultant image were plotted to a histogram and peak locations representing the resin, fibers, and voids were identified. A threshold was placed to segregate and contour the voids, creating an image of white void areas on a black background. The porosity of the imaged location is then calculated by taking the contoured area (number of white pixels) to the entire image size (total pixel area of the image). This calculation was repeated across the sample thickness to provide an analysis of microstructure development and to validate the finite element model discussed above.

SCANNING ELECTRON MICROSCOPY (SEM)

Regions and details of interest that were too small to analyze with optical microscopy were investigated using a Phenom ProX scanning electron microscope. Samples intended for SEM analysis were left unpolished allowing for the imaging of raw cross-sectional details. A gold thin film was deposited onto the samples using a sputter coater due to the low conductivity of the composite.

RAMAN SPECTROSCOPY

The chemical structure, phase, and polymorphy of the composite were examined using a Renishaw inVia Raman microscope. Mounted samples of the ½'' pyrolyzed laminate were analyzed to investigate the changes in the material's molecular structure under varying temperatures, as reflected in the corresponding Raman spectra. Pyrolyzed samples were analyzed at different spots across the thickness to identify any potential changes in the microstructure due to possible gradients in the degree of of pyrolysis.

Data obtained from the analyses was cleaned and smoothed using Python scripts developed in-house. The SciPy Python library was used to normalize each test via min-max normalization, and the resulting peaks were characterized by obtaining the associated wavenumbers and the values corresponding to the respective prominence and width.

RESULTS

Process Simulation

Using the theory-based ML + FE framework, simulations were performed to predict the temperature and weight loss (%) gradients across the thickness of the laminate. The following results show the variations obtained for laminates with

thicknesses of 1.3 cm (½'') and 2.54 cm (1'') when using a tool with thickness of 1 cm and assuming a low heat transfer coefficient at the bottom of the part.

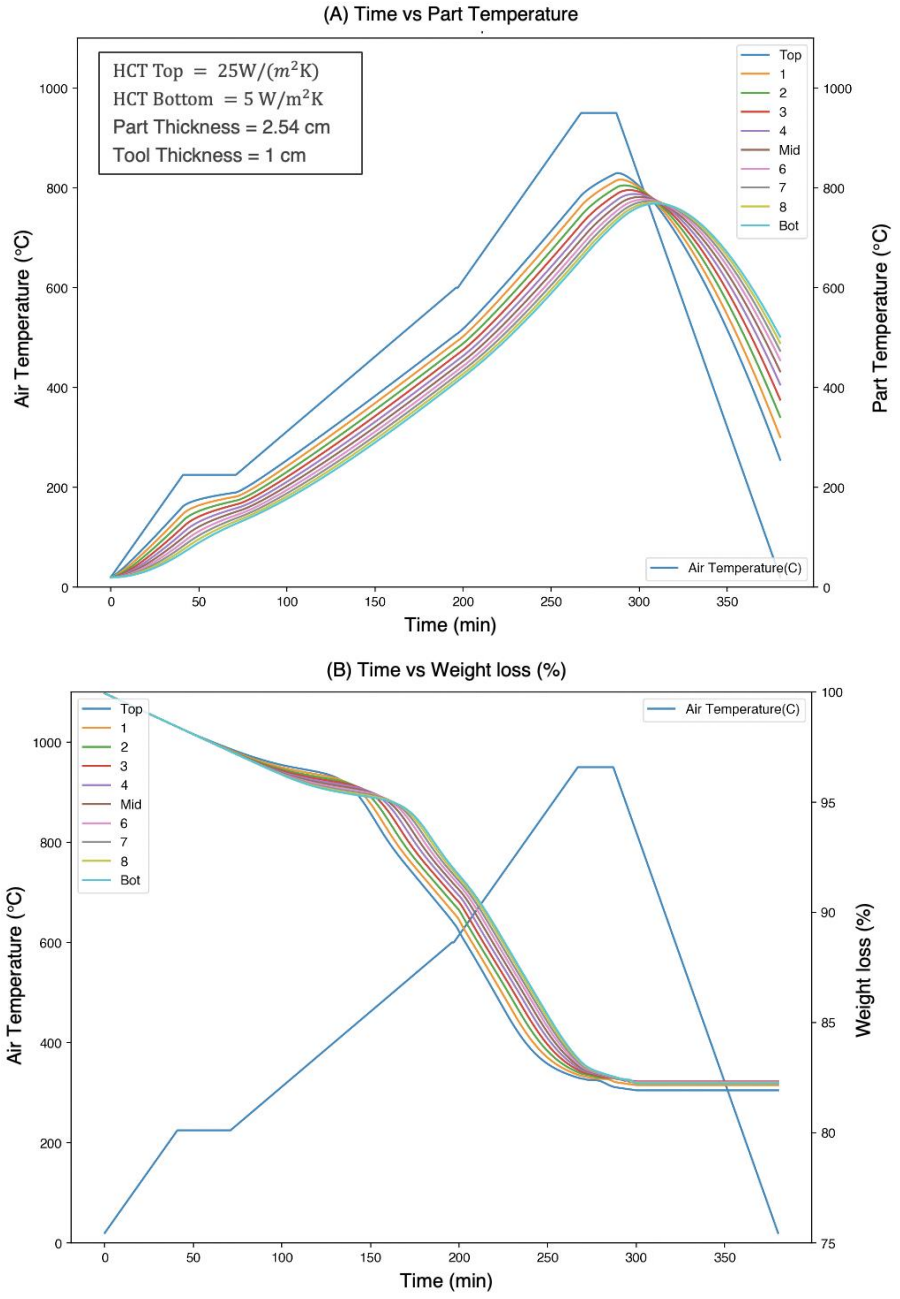

Figure 4. Temperature (A) and weight loss (%) (B) gradients across thickness for a laminate of thickness of 2.54 cm (1'') and tool thickness of 1 cm.

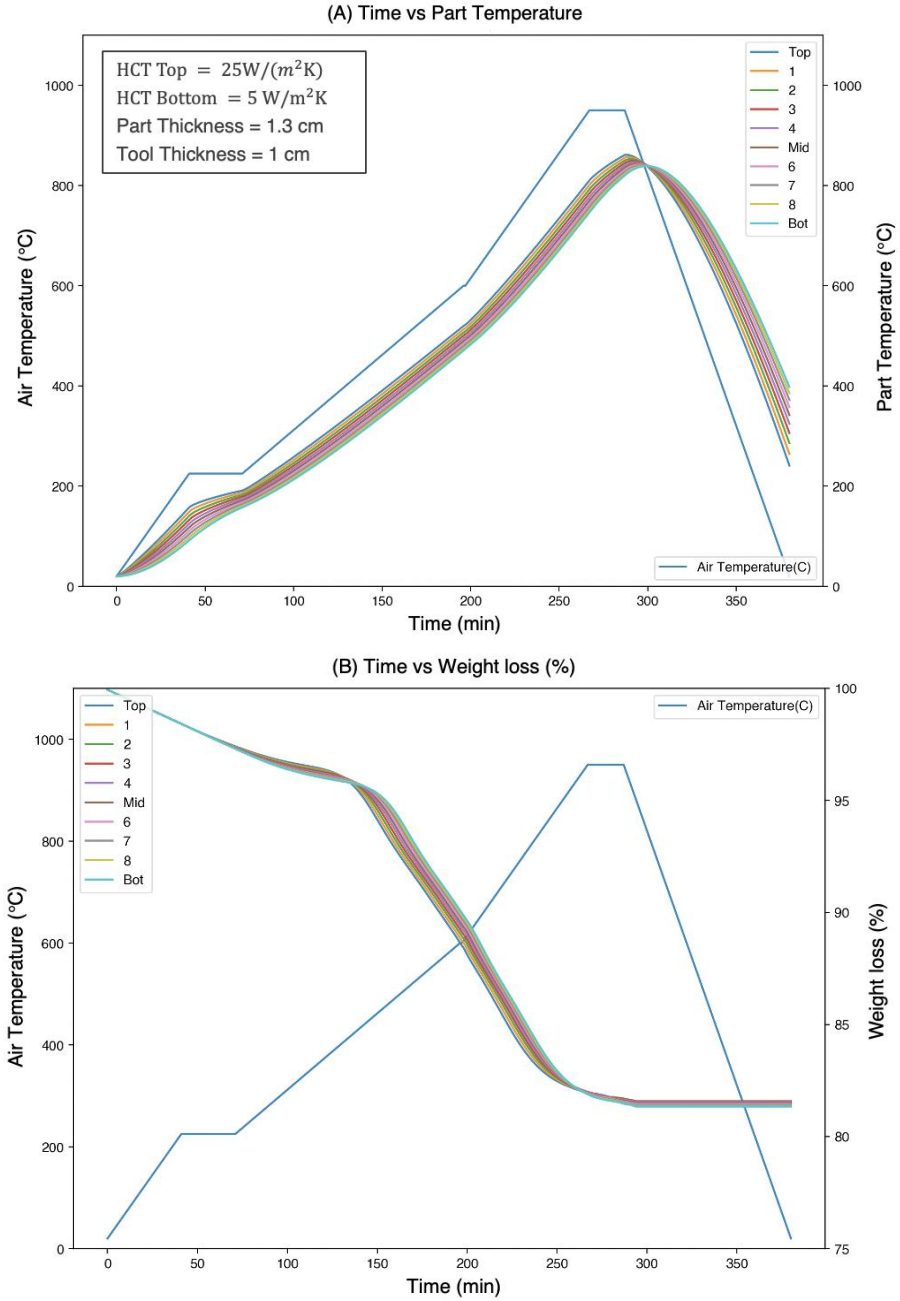

Figure 5. Temperature (A) and weight loss (%) (B) gradients across thickness for a laminate with thickness of 1.3 cm (½'') and tool thickness of 1 cm.

Variances between the minimum and maximum values of the predicted weight loss across the thickness of the part were observed to be 0.22% and 0.42% for the 1.3 cm and 2.54 cm samples, respectively. These samples had predicted average weight loss values of 18.59% and 17.86%, respectively.

Simulations were also conducted using a tool with a thickness of 0.5 cm for all laminate thicknesses to further investigate the effect of the part thickness in the weight loss gradient and compare with the results obtained experimentally. Simulation results are summarized in Tables I and II.

TABLE I. WEIGHT LOSS RESULTS OBSERVED FOR A TOOL THICKNESS OF 0.5 CM

Sample Thickness (cm)	Min WL (%)	Max WL (%)	Variance (%)	Average WL (%)
0.64	19.0	19.1	0.12	19.0
1.30	19.1	19.2	0.13	19.1
2.54	19.0	19.1	0.14	19.0

TABLE II. WEIGHT LOSS RESULTS OBSERVED FOR A TOOL THICKNESS OF 1 CM

Sample Thickness (cm)	Min WL (%)	Max WL (%)	Variance (%)	Average WL (%)
0.64	18.9	18.9	0.03	18.9
1.30	18.5	18.7	0.22	18.6
2.54	17.8	18.2	0.42	17.9

A reduction in weight loss is observed with increased thickness of both the part and tool, which can be attributed to heat and mass transfer being hindered. Figures 4(A) and 5(A) exhibit a significant increase in the temperature gradient across the thickness for the 1'' laminate, due to a potential increase of thermal lag, and decrease in the part's thermal conductivity. Physically, thicker parts may also experience slower mass transfer rates, obstructing the availability of pathways for the volatile components generated from the pyrolysis reactions. This slower mass transfer restricts the access of heat and volatiles to and from the interior regions of the part, thus affecting the resulting microstructure [7,20]. However, it should be noted that mass transfer is not simulated in the current study.

The heterogeneous distribution of temperature across the part leads to an uneven evolution of the material properties and therefore of the weight loss and degree of pyrolysis. Furthermore, using a thicker tool in direct contact with the part would reduce the effective heat transfer at the bottom of the part. As part thickness increases, this effect also appreciably increases the temperature, weight loss, and degree of pyrolysis gradients.

Model Validation

Visual examination of the optical microscopy images showed a significant increase in apparent porosity post-pyrolysis, with minimal changes noted in the fibers. Grayscale micrographs obtained from the center of the ½'' and ¼'' sample's cross-sections are shown in Fig. 6. Porosity calculation using image analysis confirmed a significant increase in the porosity of the samples after pyrolysis, as well as a usually lower porosity in the middle of the sample compared to the edges (Table III). The presented data in Table III show an average porosity of 21.1 ±0.7% (¼") and 23.1±3.1% (½") for the pyrolyzed samples and 2.0±0.2% for the cured sample. These tests showed minimal influence of thickness on the porosity of the pyrolyzed samples.

Calculating the difference between the pyrolyzed and cured samples gives a weight loss of 19.1% for the ¼" pyrolyzed sample and 21.1% for the ½" sample. This is a close match to the 19% weight loss obtained by the ML-FE model for the same sample (error < 3%). This correlation serves as the validation of the model.

TABLE III. POROSITY MEASUREMENTS FOR CURED AND PYROLYZED SAMPLES AT VARYING THICKNESSES.

Sample	Part Top (%)	Part Middle (%)	Part Bottom (%)	Average (%)
½" Cured	2.2	2.0	1.6	2.0 ± 0.2
¼" Pyrolyzed	21.0	20.3	22.1	21.1 ± 0.7
½" Pyrolyzed	27.4	20.4	21.5	23.1 ± 3.1

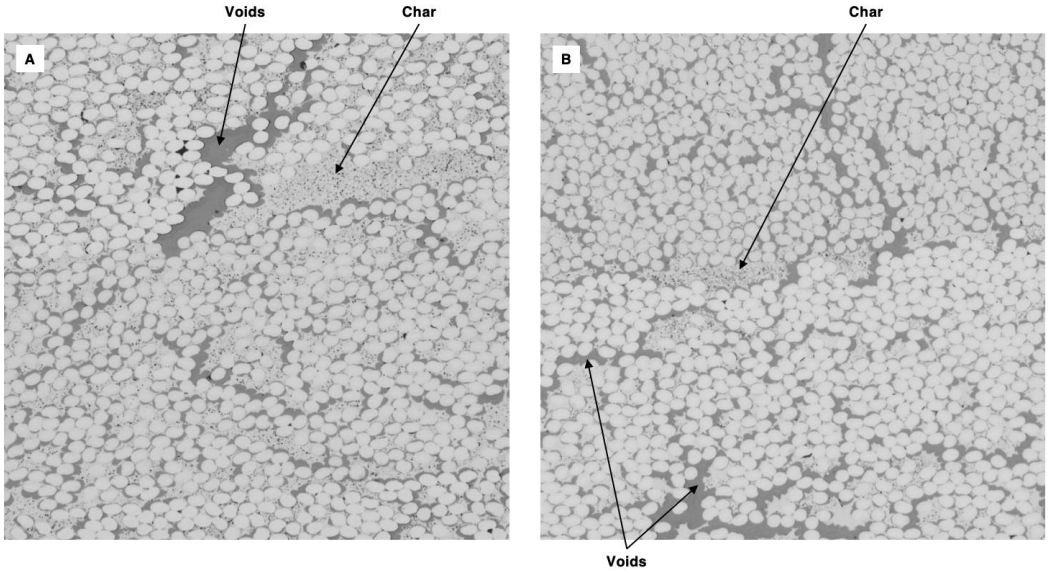

Figure 6. Grayscale micrographs obtained from the center of the pyrolyzed ¼'' (A) and pyrolyzed ½''(B) laminate samples.

Microstructure Development

SEM images were used to confirm the occurrence of resin shrinkage after pyrolysis as well as to investigate any regions that had notable artifacts.

Results obtained from Raman spectroscopy were analyzed to study the structural changes associated with the degree of pyrolysis in the samples. These results were compared with existing literature data for similar systems. The progression of the pyrolytic process of carbon-based resins is marked by the emergence of the characteristic bands associated with the D and G/D' modes, which indicate distorted and graphitic structures. These bands are observed in the Raman shift at approximately 1350 and 1600 wave numbers, respectively [6,21]. As the degree of pyrolysis advances, an increase in the D-mode is expected as it is an indication of an increase in molecular disorder associated with the formation of polymeric carbon [21].

The Raman spectra obtained from different positions across the thickness of the pyrolyzed sample are shown in Figure 7. Results are consistent with those expected for a similar material based on the kinetic theory.

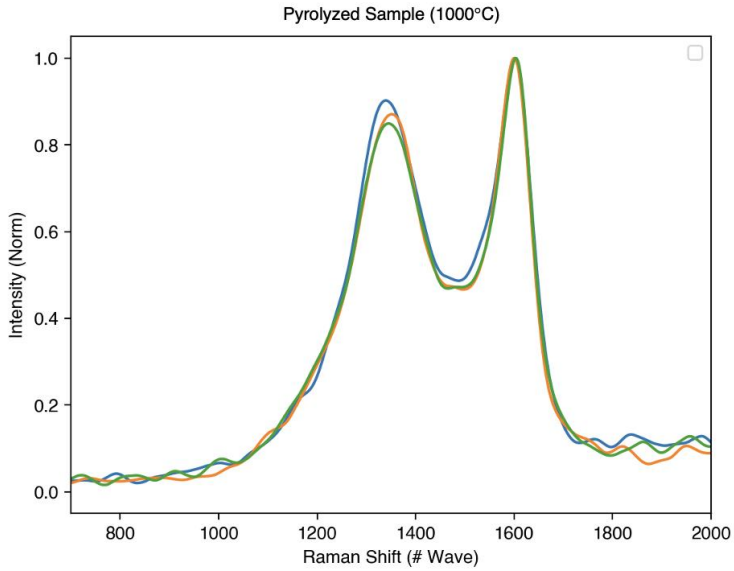

Figure 7. Raman spectra obtained from various positions along the thickness of the pyrolyzed ½" laminate sample.

CONCLUSIONS

Theory-guided machine learning methods can be successfully combined with finite element analysis to accurately characterize the pyrolysis kinetics for high-temperature composites and simulate the material's behavior under varying processing conditions and part thicknesses. Results presented in this study were achieved by only conducting a total of 7 TGA experiments for ML-model training and optimization, and 2 pyrolysis runs using the tube furnace setup for validation. This demonstrates that the presented framework enables a significant reduction in experimental efforts.

It is important to acknowledge potential sources of errors that may arise from assumptions made during the calculations of the material properties evolution throughout the process. These assumptions include the estimation of density and thermal conductivity based on the weight loss evolution. Future work will be conducted to enhance the model's accuracy, and validation for different processing conditions and thicknesses.

AKNOWLEDGMENTS

This research was sponsored by Lockheed Martin Corporation.

REFERENCES

1. Torres-Herrador, F., Coheur, J., Panerai, F., et al. 2020. “Competitive kinetic model for the pyrolysis of the Phenolic Impregnated Carbon Ablator.” *Aerospace Science and Technology*, 100. DOI https://doi.org/10.1016/j.ast.2020.105784
2. Tzeng, S. and Y. Chr. 2002. “Evolution of microstructure and properties of phenolic resin-based carbon/carbon composites during pyrolysis”. *Materials Chemistry and Physics*, 73(2-3): 162-169. DOI https://doi.org/10.1016/S0254-0584(01)00358-3.
3. Nam, J.-D and Seferis, J. 1993. “Volatile Evolution in Thermoset Composites from Processing to Degradation.” *Science and Engineering of Composite Materials*, 2. DOI 10.1515/SECM.1993.2.3.211.
4. Torres-Herrador, F., Eschenbacher, A., Coheur, J., Blondeau, J., Magin, T. E. and K. M. van Geem. 2021. “Decomposition of carbon/phenolic composites for aerospace heatshields: Detailed speciation of phenolic resin pyrolysis products”. *Aerospace Science and Technology*, 119. DOI https://doi.org/10.1016/j.ast.2020.105784.
5. Trick, K. A., Saliba, T. E., and S. S. Sandhu. 1997. “A Kinetic Model of the Pyrolysis of Phenolic Resin in Carbon/Phenolic Composite”. *Carbon*, 35(3): 398-401. DOI https://doi.org/10.1016/S0008- 6223(97)89610-8.
6. Ko, T. H., Kuo, W. S., and Y.H. Chang. 2000. “Raman study of the microstructure changes of phenolic resin during pyrolysis”. *Polymer Composites*, 21(5): 745–750. https://doi.org/10.1002/pc.10229
7. Rim Choe, C., and K. Hee Lee. 1992. Effect of Processing Parameters on the Mechanical Properties of Carbonized Phenolic Resin. In *Prmtcd I*, 30(2).
8. Portales, P.P., Gray, A., and N. Zobeiry. (2023). “A Novel Framework for Accelerated Characterization of Pyrolysis Kinetics of High-Temperature Composites Using Theory-Guided Probabilistic Machine Learning” presented at the 2023 SSDM Conference, June 19-21, 2023.
9. Portales, P.P., Gray, A., Cheng, R. and N. Zobeiry. (2023). “A Machine Learning-Based Accelerated Pyrolysis Characterization and Optimization of High-Temperature Composites” presented at the 2023 SAMPE Conference, April 17-20, 2023.
10. Schellhase, K., Brushaber, R., Wu, H., et al. May 2016. “Development of New Thermal Protection Systems Based on Polysiloxane/Silica Composites: Properties Characterization I.” *SAMPE Conference Proceedings*. Long Beach, CA.
11. Schellhase, K., Koo, J., Buffy, J., et al. May 2017. “Development of New Thermal Protection Systems Based on Polysiloxane/Silica Composites: Properties Characterization II.” *SAMPE Conference Proceedings.* Seattle, WA, May 22-25, 2017. DOI https://doi.org/10.1016/j.carbon.2009.09.036
12. Wynn, M., and N. Zobeiry. 2023. “Investigating the Effect of Temperature History on Crystal Morphology of Thermoplastic Composites Using In Situ Polarized Light Microscopy and Probabilistic Machine Learning”. *Polymers*, 15(1). DOI https://doi.org/10.3390/polym15010018.
13. Zobeiry, N., and K.D., Humfeld. 2021. “A physics-informed machine learning approach for solving heat transfer equation in advanced manufacturing and engineering applications.” *Engineering Applications of Artificial Intelligence*, 101, 104232. DOI https://doi.org/10.1016/j.engappai.2021.104232
14. Zobeiry, N., Johannes R., and V. Reza. 2020. "Theory-guided machine learning for damage characterization of composites." *Composite Structures*, 246, 112407. DOI https://doi.org/10.1016/j.compstruct.2020.112407
15. Jiang, H., Wang, J., Wu, S., et al. 2010. “Pyrolysis Kinetics of Phenol-Formaldehyde Resin by Non-isothermal Thermogravimetry”. *Carbon*, 48: 352-358.
16. Kumar, O.D., Viju, D., and R. Vinu. 2021. “Fast Pyrolysis Kinetics of Lignocellulosic Biomass of Varying Compositions”. *Energy Conversion and Management: X*, 10:100071. DOI https://doi.org/10.1016/j.ecmx.2020.100071.
17. Beckers, T. 2021. “An Introduction to Gaussian Process Models”. DOI https://doi.org/10.48550/arXiv.2102.05497.
18. Freed, Y., Salviato, M., and Zobeiry, N. 2022. “Implementation of a probabilistic machine learning strategy for failure predictions of adhesively bonded joints using cohesive zone

modeling". *International Journal of Adhesion and Adhesives,* 118, 103226. DOI https://doi.org/10.1016/j.ijadhadh.2022.103226.

19. Freed, Y., Zobeiry, N., and Salviato, M. 2022. "Development of aviation industry-oriented methodology for failure predictions of brittle bonded joints using probabilistic machine learning." *Composite Structures*, 297, 115979. DOI https://doi.org/10.1016/j.compstruct.2022.115979.
20. Hoyt, J.J. 2011. *Phase Transformations.* McMaster University, pp. 1-31.
21. Evelyn, A.L., Ila, D., and G.M. Jenkins. (1994). "RBS and Raman spectroscopy study of heat-treatment effect on phenolformaldehyde resin". *Nuclear Instruments and Methods in Physics Research B,* 85:861-863.
22. Sykes, G. F.1967. "Decomposition Characteristics of a Char- Forming Phenolic Polymer Used for Ablative Composites." NASA Technical Note 19670008814, NASA Langley Research Center Hampton, VA. DOI https://ntrs.nasa.gov/search.jsp?R=19670008814
23. Liu, C. L., Dong, W.-S., Song, J. R., and L. Liu. 2007. "Evolution of microstructure and properties of phenolic fibers during carbonization." *Materials Science and Engineering A,* 459(1–2): 347–354. DOI https://doi.org/10.1016/j.msea.2007.02.067
24. Grujicic, M., Zhao, C. L., Dusel, E. C., Morgan, D. R., Miller, R. S., and D.E. Beasley. 2006. "Computational analysis of the thermal conductivity of the carbon-carbon composite materials". *Journal of Materials Science*, *41*(24): 8244–8256. https://doi.org/10.1007/s10853-006-1003-x
25. Li, Z., Deng, L., Kinloch, I. A., and R.J. Young. (2023). "Raman spectroscopy of carbon materials and their composites: Graphene, nanotubes and fibres". In *Progress in Materials Science*, 135. Elsevier Ltd. https://doi.org/10.1016/j.pmatsci.2023.101089